Supporting Information

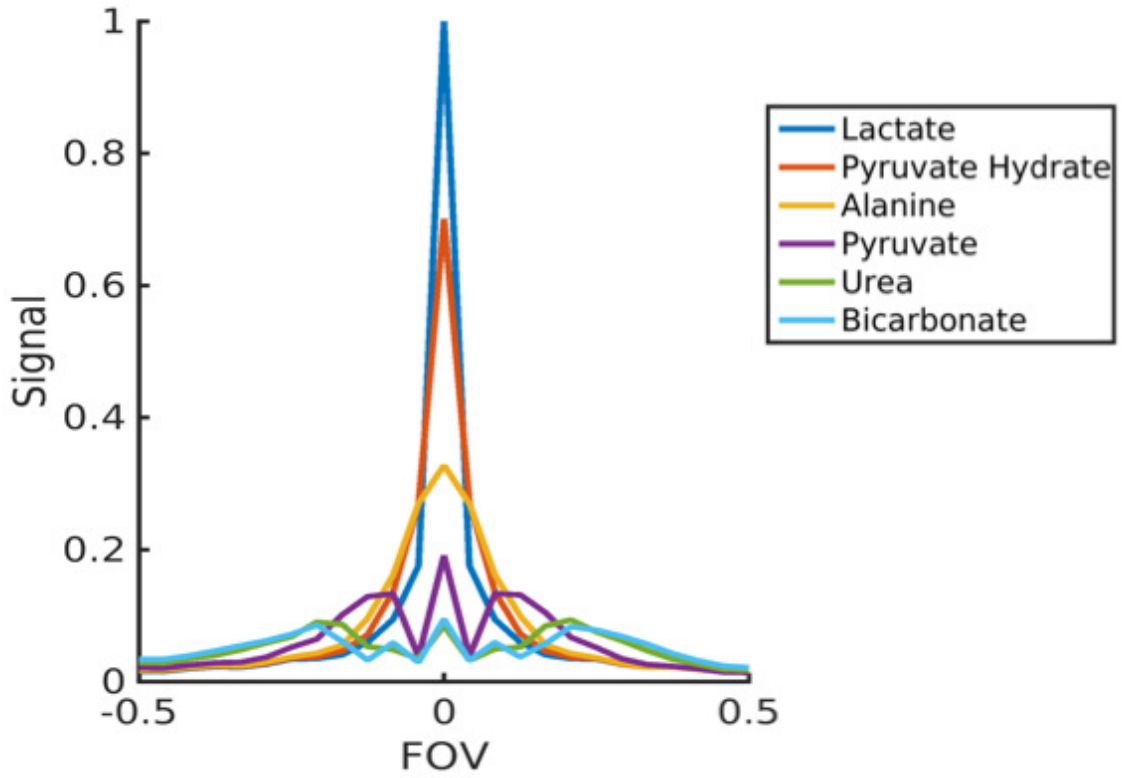

Supporting Information Figure S1: Simulations of off-resonance PSF of the interleaved spiral readouts (4 interleaves, 3.8ms for each interleaf) used in this study. Frequencies of metabolites are Lactate = 0Hz, Pyruvate Hydrate = -128Hz, Alanine = -210Hz, Pyruvate = -395Hz, Urea = -635Hz, Bicarbonate = -717Hz.

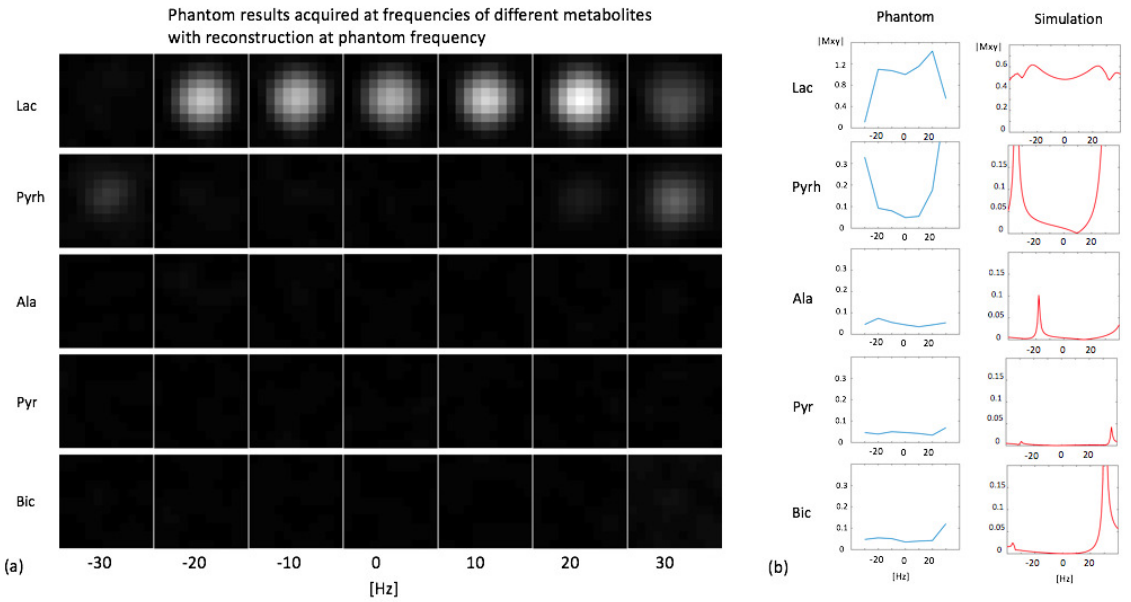

Supporting Information Figure S2: Validation of the MS-3DSSFP sequence on a ^{13}C-enriched sodium bicarbonate phantom (T1 $\sim=$ 26s, T2 $\sim=$ 1.5s). ^{13}C images were acquired with a center frequency offset, both at excitation and at acquisition, by 0Hz, 128Hz, 210Hz, 395Hz, and 717 Hz relative to the phantom frequency, to mimic the images of lactate ("Lac"), pyruvate hydrate ("Pyrh"), alanine ("Ala"), pyruvate ("Pyr") and bicarbonate ("Bic"), respectively. At the frequency of each metabolite, ^{13}C images were also acquired with small frequency offsets from -30 to 30 Hz with a step of 10Hz. Acquired data were always demodulated to the phantom frequency so that reconstructed images wouldn't be affected by blurring artifacts due to off-resonance reconstruction. All ^{13}C images were acquired at $8 \times 8 \times 20$mm and reconstructed at $4 \times 4 \times 20$mm. The mean value of the phantom area for each image is normalized by the value of the lactate image at zero frequency offset and plotted in graph (b). Simulation results from Figure 2 are also displayed here for comparison.

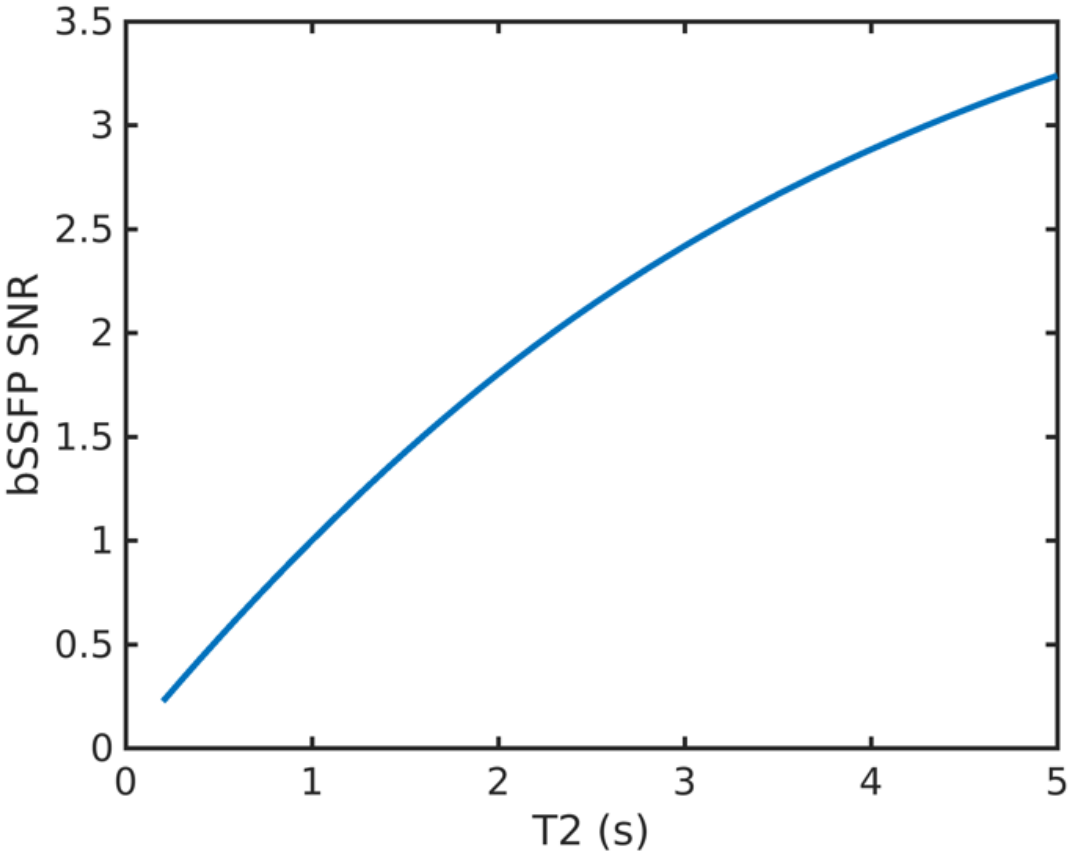

Supporting Information Figure S3: Simulation of bSSFP SNR as a function of T2, normalized to SNR is 1 when T2 is 1s. Simulation parameters include T1 = 30s, TR 15.3ms, # of time points 30, # of RF pulses 64.

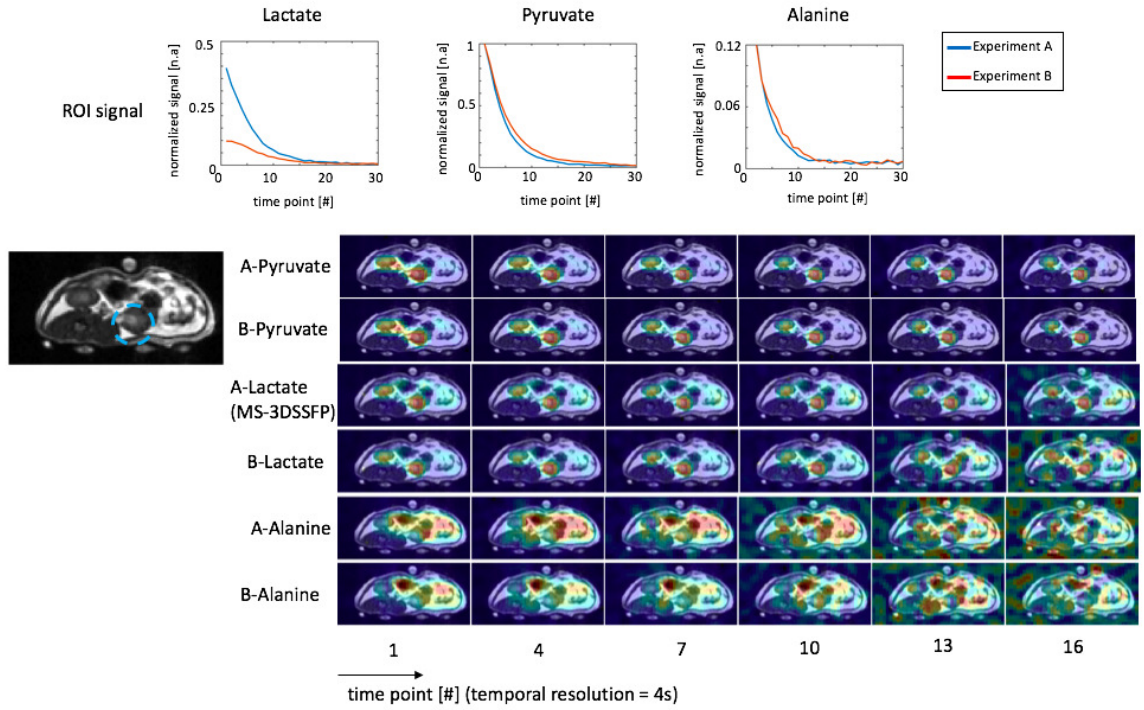

Supporting Information Figure S4: Dynamic images and ROI signal curves of a rat kidney slice of the experiments described in Figure 4. Each image is displayed to its own maximum signal to visualize metabolites at all time points. All ROI signals were divided by corresponding noise signals and then divided by the highest value of the pyruvate dynamic curve.

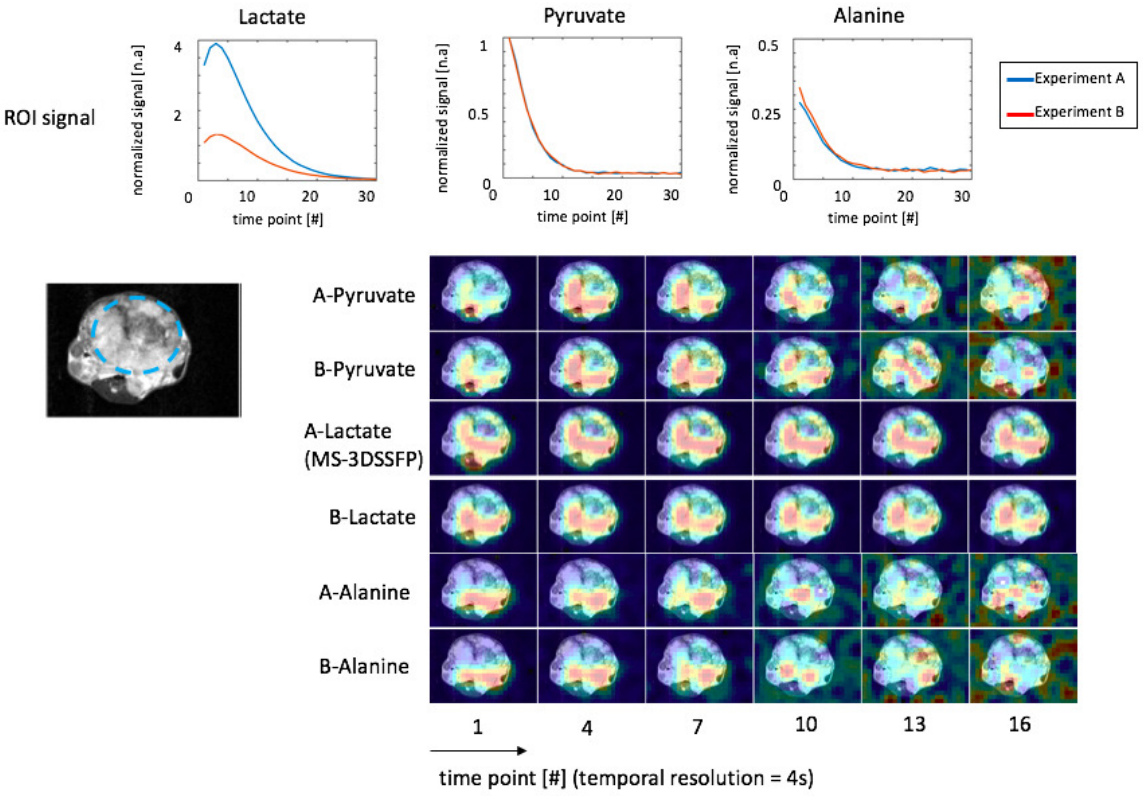

Supporting Information Figure S5: Dynamic images and ROI signal curves of a TRAMP mouse tumor slice of the experiments described in Figure 5. Each image is displayed to its own maximum signal to visualize metabolites at all time points. All ROI signals were divided by corresponding noise signals and then divided by the highest value of the pyruvate dynamic curve.

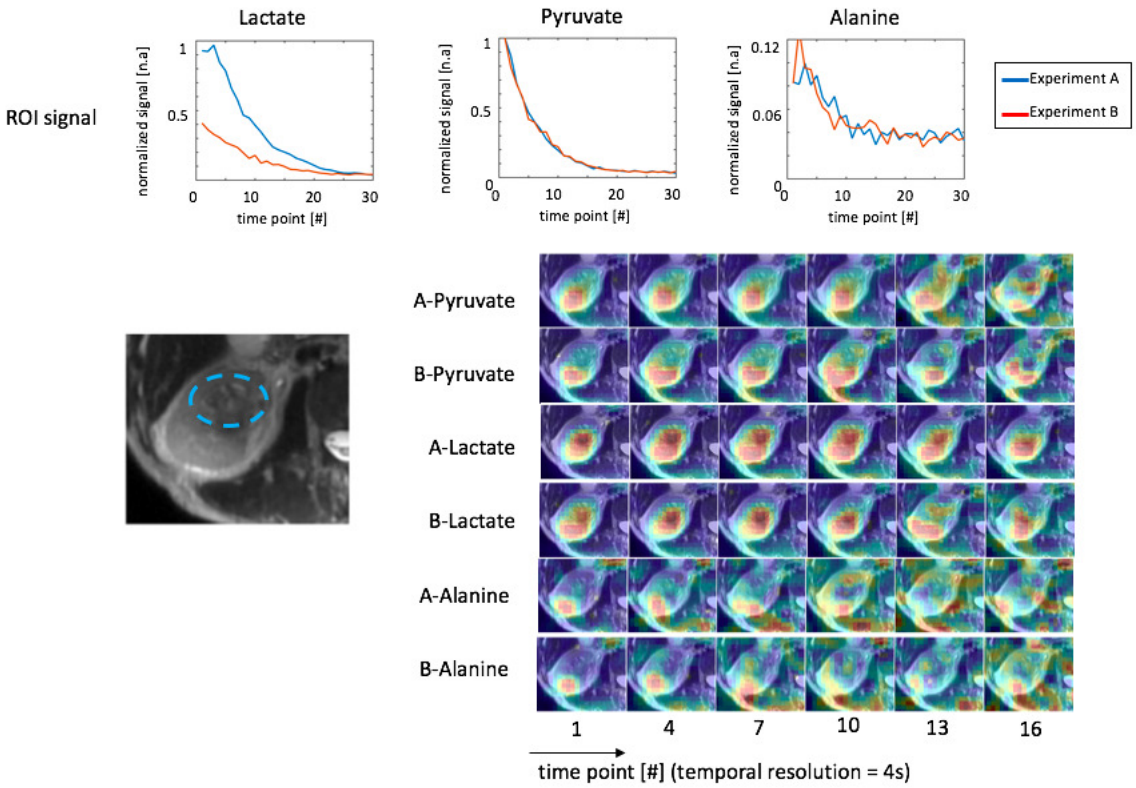

Supporting Information Figure S6: Dynamic images and ROI signal curves of a human renal tumor slice of the experiments described in Figure 6. Each image is displayed to its own maximum signal to visualize metabolites at all time points. All ROI signals were divided by corresponding noise signals and then divided by the highest value of the pyruvate dynamic curve.

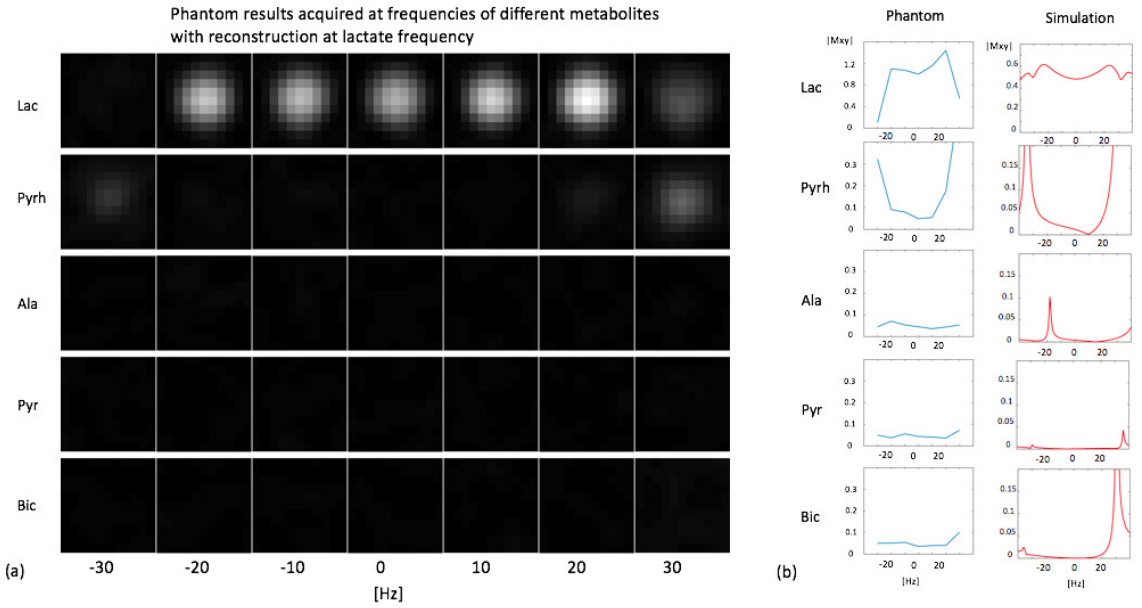

Supporting Information Figure S7: ^{13}C images of Supporting Figure S2 were displayed without applying demodulation, meaning reconstruction frequency was the same as excitation frequency. This is how reconstruction was performed in all in vivo experiments - reconstruction was always performed at the lactate frequency. This figure validates the combined effects of excitation profiles and blurring artifacts caused by spiral readouts.